FEBS Letters 356 (1994) 267–271

FEBS 14909

Covalent anchoring of proteins onto gold-directed NHS-terminated self-assembled monolayers in aqueous buffers: SFM images of clathrin cages and triskelia

Peter Wagner[a,*], Peter Kernen[a], Martin Hegner[a,b], Ernst Ungewickell[c], Giorgio Semenza[a]

[a]*Department of Biochemistry, Swiss Federal Institute of Technology, ETH Zentrum, CH 8092 Zurich, Switzerland*
[b]*Institute of Physics, University of Basle, CH 4056 Basle, Switzerland*
[c]*Department of Pathology, Washington University, St. Louis, MO 63110, USA*

Received 15 November 1994

Abstract *N*-Hydroxysuccinimide-terminated self-assembled monolayers with linear $(CH_2)_{10}$ chains were prepared on ultraflat Au(111) surfaces from dithio*bis*(succinimidylundecanoate). These monolayers, which are covalently chemisorbed to gold via thiolate bonds, form a highly reactive amino-group specific carpet at the liquid–solid interface. Proteins bind to it covalently in aqueous buffers under mild conditions; this provides a (general) procedure for protein immobilization for scanning probe microscopy. Using this technique, we have obtained what we believe are the first scanning force microscopy images of clathrin cages and of their in situ disassembly, yielding typical triskelia under non-denaturing conditions.

Key words: Atomic force microscopy; Scanning force microscopy; Gold; Self-assembled monolayer; *N*-Hydroxysuccinimide; Clathrin; Triskelion

1. Introduction

Scanning probe microscopy (SPM) potentially allows direct imaging of individual macromolecules under 'physiological' conditions, i.e. undenatured, in aqueous buffers, and also in the presence of appropriate ligands or effectors; for reviews see [1–5]. Even if this has to be paid for with a lower resolution, as compared to that of high-resolution electron microscopy (and of course also to that of SPM of many inorganic and organic materials), SPM should in principle allow structure–function studies to be carried out on native biological objects, particularly when major structural changes are involved.

One of the conditions to be fulfilled for SPM imaging of macromolecules in aqueous solutions is that they should be firmly anchored on appropriate substrates and thus not be displaced by the tip while scanning. Such substrates should be flat, i.e. featureless over large areas, be chemically inert, yet allow fixation of the objects. Mere electrostatic interactions, for example, would severely limit the conditions under which biological objects can be eventually investigated (e.g. only at low ionic strength or within a limited pH range). A variety of crystalline or amorphous substrates have been used to date, having different chemi- or physisorption properties. The substrates mostly used are mica, glass, silicon wafers, highly oriented pyrolytic graphite (HOPG), and gold.

Mica has excellent flatness. It binds biomolecules via electrostatic interactions (thus with the limitations indicated above), also after appropriate derivatization [6–10]. Glass can be derivatized to make it bind proteins covalently via silanization [11,12]; it has the additional advantage of allowing imaging of the very same sample by both SPM and other techniques requiring a transparent support. Also HOPG (if used underivatized, but see [13]), binds macromolecules by way of weak electrostatic or 'adsorption' forces (and, moreover, it has fallen into, perhaps excessive, disrepute when it was shown to yield artifactual images mimicking DNA [14,15]). Gold is, we think, an even more promising substrate: it is inert against O_2, yet it can form very stable covalent Au–thiolate bonds [16–19]. Additional advantages of gold are related to its conductivity: it allows STM imaging and also potentiostatic deposition of charged macromolecules. We have recently worked out a simple and reproducible procedure to prepare ultraflat Au(111) surfaces (template-stripped gold, TSG) with a mean roughness as small as 2–5 Å over more than 25 μm^2 [20,21], thus overcoming the serious drawbacks of the irregular topography (on μm scale) of epitaxially grown or of other gold surfaces, as prepared by established procedures (for a comparative review until 1992, see [22]).

Some biomolecules may bind to these gold surfaces without additional treatment (e.g. via pre-existing thiol groups, or physisorption), but the two main all-purpose routes are: (i) introducing (extra) thiol groups into the biomolecule (e.g. DNA [23], see also [24]), proteins (via Traut's reagent: [25] and unpublished data from our group), phospholipids [26]), or (ii) formation of derivatised gold-directed self-assembled monolayers (SAM) onto these ultraflat Au(111) surfaces with subsequent non-covalent [27] or covalent anchoring of biological macromolecules (see below).

Here we deal with the latter approach. Hydrophobic thiols (e.g. dodecanethiol) easily form regular monolayers on epitaxially grown gold surfaces (e.g. [16–19]) with a commensurate $(\sqrt{3} \times \sqrt{3})$ R30° overlayer structure. Au(111) directs the thiolates to form two-dimensional arrays, which are further stabilized by their lateral hydrophobic interactions. The ultraflat Au(111) surfaces mentioned above [20] are exquisitely flat templates onto which to build very regular, extended monolayers, for

*Corresponding author. Fax: (41) (1) 632 1269.

Abbreviations: SPM, scanning probe microscopy; SFM, scanning force microscopy; STM; scanning tunneling microscopy; SAM, self-assembled monolayer; NHS, *N*-Hydroxysuccinimide; TSG, template-stripped gold; DSU, dithio*bis*(succinimidylundecanoate); HOPG, highly oriented pyrolytic graphite.

0014-5793/94/$7.00 © 1994 Federation of European Biochemical Societies. All rights reserved.
SSDI 0014-5793(94)01296-2

example of palmitoyl-*N*-cysteamine [21], or of ω-functionalized thiols. If the ω-substituent is a highly reactive group, it can act as the anchoring site, docking proteins onto the monolayer carpet. We have used here dithio*bis*(succinimidylundecanoate) (DSU). It readily forms regular and extended monolayers; the *N*-hydroxysuccinimidyl groups, which are exposed at the monolayer-water interface, react with amino groups under very mild conditions (pH ~6.5–7.5).

In this paper we focus on clathrin and its association states. This protein forms the regular polyhedral surface lattice of clathrin-coated vesicles, which are involved in intracellular protein transport. This function involves the reversible association of three-legged clathrin protomers (triskelia), composed of three heavy and three light chains, into regular coat structures. In vitro purified clathrin triskelia associate in the absence of membranes into empty cages which are very similar to the surface lattice of coated vesicles. Both triskelia and cages have been extensively characterized by electron microscopy [28,29].

This system was chosen because (i) cages and triskelia differ considerably in size and shape, and would thus be easily distinguished by SFM, (ii) clathrin is readily purified and the two association states are interconvertible by simple and established manipulations [30], thus enabling in situ studies of dynamic events in the nanometer range, (iii) clathrin contains enough lysine residues for immobilization, and (iv) our understanding of the dynamics of clathrin assembly and disassembly is likely to improve by using SFM.

2. Materials and methods

2.1. Materials and instrumentation

Clathrin coated vesicles were prepared from bovine brains according to [31], and clathrin (cages) were purified according to [30]. All chemicals and solvents were commercial grades of highest purity. Gold, mica, Si-wafer and epoxy-glue Epo-tek No. 377 were purchased as reported previously [20]. Synthesis of dithio*bis*(succinimidylundecanoate) was carried out via oxidation of the Bunte salt of 11-bromoundecanoic acid (Wagner et al., in preparation).

Scanning force microscopy was carried out on a NanoScope III from Digital Instruments Inc. (Santa Barbara, CA, equipped with an E-scanner with a 10×10 μm scan range), and scanning tunneling microscopy on a home-built system. For SFM we used microfabricated monocrystalline silicon tips (with force constants ranging from 0.06 to 0.17 N/m, purchased from LOT, Darmstadt, Germany), and for STM mechanically cut Pt/Ir tips.

2.2. Preparation of template-stripped gold surfaces (TSG)

According to our procedure described in [20], gold was deposited 200 nm thick onto freshly cleaved, preheated (300°C) ruby muscovite mica sheets. After glueing onto a Si-wafer piece using the epoxy glue, the mica was removed by immersing the [Si–epoxy glue–gold–mica] multilayer into tetrahydrofuran. This resulted in exposure of the ultraflat Au(111) surfaces (TSG).

2.3. Formation of the NHS-SAM

The monolayer was prepared on these ultraflat Au surfaces by immersing the TSG in a 1 mM solution of DSU in acetone for 2 h at room temperature. After rinsing with acetone, the NHS-terminated monolayer was dried under a stream of nitrogen and immediately used for the immobilization step.

2.4. Protein immobilization and SFM imaging

The general procedure for immobilizing amino groups containing biomolecules was as follows: 50 μl of the protein solution (amine free buffers are mandatory) at a concentration of 1 μg/ml were placed on a piece of parafilm; a TSG platelet was carefully put upside down onto the drop. After 1 h the platelet, now carrying the covalently immobilized biomolecules, was rinsed with 2 ml buffer solution and placed into the fluid cell of the NanoScope. The buffer used here in the immobilization step and in the first imaging (see Fig. 3A below) was 100 mM MES (pH 6.5), 1 mM EGTA, 0.5 mM $MgCl_2$ and 0.05% NaN_3. Subsequent injection of 200 μl of 0.5 M Tris-HCl (pH 7) into the fluid cell nearly completely exchanged the buffer, which triggered the in situ disassembly of the immobilized cages.

Image acquisition in the constant-force imaging mode was carried out in the buffers indicated. The proteins were never left to dry at any stage. Forces were in the range of approximately 1 nN and scan speeds were lower than 1 μm/s. The piezo scanners were calibrated in the *x* and *y* dimensions, by using a Si calibration standard with a periodicity of 200 nm, and in the *z*-dimension from the known monoatomic step heights of Au(111). All images shown in the following are based on unfiltered data.

3. Results and discussion

Ultraflat gold substrates were prepared and characterized as reported previously in detail [20,21]. NHS-SAM spontaneously formed onto them from DSU by self-assembly in a rather straight-forward manner (see section 2). In Fig. 1 the resulting complete multilayer system is shown, consisting of NHS-SAM–Au(111)–epoxy glue–Si(100). The NHS-SAM covered the

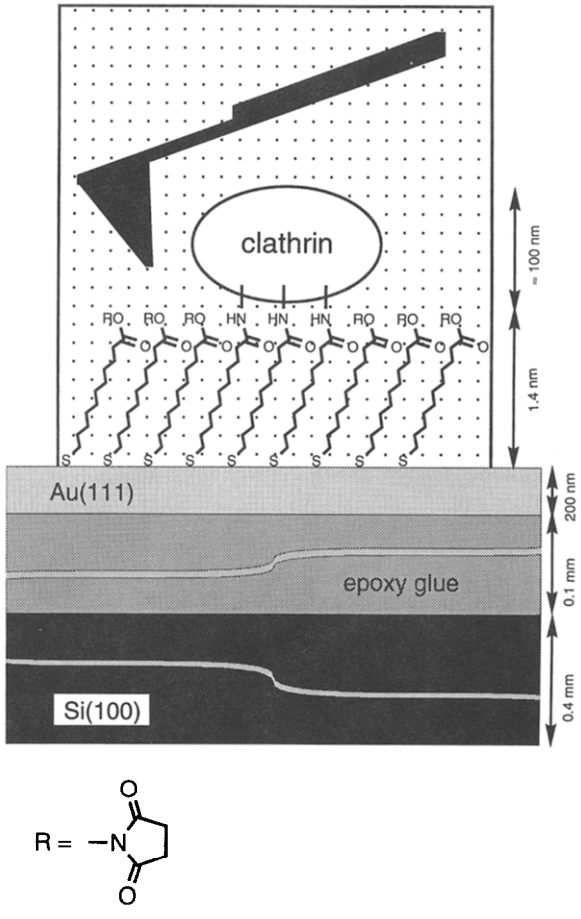

Fig. 1. A schematic view of the experimental set-up developed in the present paper for SPM imaging of a protein (not to scale). (Some of) the amino groups of clathrin have reacted with the NHS-activated carboxylic acid groups at the water–solid interface of a self-assembled monolayer. The monolayer is covalently bound via S-Au bonds to ultraflat template-stripped gold (TSG) surfaces (roughness, 2–5 Å over 25 μm^2) [20]. The Au(111) film is supported by a Si(100) wafer, to which it is glued via a special epoxy resin (Epo-tek).

atomically flat gold terraces completely and exhibited the depressions (see an STM image in Fig. 2), which are characteristic of this type of monolayers (see e.g. [32,33]).

Using this immobilization system we have now anchored a number of proteins and organelles onto this SAM for imaging by SPM methods in aqueous buffers. In all cases the biomolecules were immobilized stably and reproducibly, providing SFM images with satisfactory quality (data not shown).

Fig. 3A is a top-view SFM image of immobilized clathrin cages. Clearly, the cages were firmly immobilized to the underlying monolayer: they were not swept away by the tip during scanning over several hours. Even increased loading forces (to 10 nN) did not alter the distribution pattern of the cages in the scan area. Also, the cages were not demolished or disassembled by the tip, since no single triskelia were found. If triskelia would have been released from the cages they should have bound to the monolayer because the hydrolysis half-time of the *N*-hydroxysuccinimidyl groups at pH 6.5 is long enough to retain sufficient binding capacity over the time course of the experiment. Changing the concentration of cages in the immobilization buffer led to corresponding changes in their density in the images obtained (not shown). The diameters of the cages centered around 155 ± 21 nm ($\bar{x} \pm$ S.E.M., $n = 86$), which was larger than the diameters as obtained from electron microscopy (e.g. [28,29]). The difference between SFM and electron microscopy was most likely due to the convolution of the geometry of the tip (experiments are presently in progress using internal topographic standards and image processing methods to eliminate tip induced broadening). Heights were in the range of 16 ± 6 nm ($n = 86$) due to a compression of about 80%. Structural details of the cages, such as hexagonal or pentagonal pores, were not resolved, i.e. the lateral resolution was lower than that in electron microscopy. This was not unexpected for various reasons, e.g. the flexibility and nature of the sample in aqueous media, the shape of the tip, the tip-induced sample perturbation during the scan, deformations of the sample due to probe and hydration forces, etc. These differences from electron micrographs were the tribute to be paid for keeping the cages in their native state.

The non-denaturing conditions enabled us to carry out the following experiment: changing to a buffer system leading to in vitro disassembly within a short time period, should allow us to visualize the disintegration of the cages. Indeed, a few minutes after the injection of the disassembly-inducing buffer, the cages had changed size and shape. Fig. 3B shows an SFM image captured 10 min after changing to Tris buffer: the cages had now changed to porous looking structures exhibiting much lower *z*-heights (approximately 2 nm). Widths were similar to the cages in Fig. 3A. In this intermediate basket-like stage, the cages had apparently disassembled except in their bottom parts (some 'baskets' are zoomed in Fig. 3C). The kinetics of cage disassembly observed at the liquid–solid interface were much slower than those in bulk solutions; possibly due to a number of factors: multiple covalent bonds to the underlying SAM; interface effects, etc. Whatever the reasons for this difference, the original, SAM-anchored cages in Fig. 3A were obviously still in a native 'functional' state, i.e. they could disassemble under appropriate conditions.

The filaments (see Fig. 3B, black arrow) attached to nearly unscathed cages (having *z*-dimensions comparable to those of the original cages in Fig. 3A) were probably clathrin molecules imaged while being released. 'Snapshots' such as this were observed solely under conditions leading to disassembly; hence, they were not artefacts due, e.g., to the scanning tip.

Images taken after 2 h (Fig. 3D) showed that the baskets had disassembled completely, yielding individual clathrin triskelia only. Most of them were not regularly spread out with the three legs at an angle of 120°, probably due to them being immobilized via unfavourable or too few anchoring points. The latter mechanism is probably the more important, because the triskelia had reacted with the underlying monolayer while still wedged in the scaffolding of the cages. (Occasional holes in the gold film were the cause of both the black spots and the horizontal bright deflections of the stylus seen in Fig. 3D.)

The magnification of a triskelion is shown in Fig. 3E. Its dimensions compare well with those obtained from electron microscopy with each of the legs measuring 45 nm in length. The globular amino-terminal domains with diameters of about 12 nm, are also clearly discernible. This domain appears to be connected via a flexible 6.5–10 nm long linker to the stiffer distal domain. Missing is, however, the kink which has been seen frequently in electron micrographs of rotary shadowed triskelia. It usually divides the triskelion leg into proximal (17 nm) and distal (22 nm) parts [34,35]. Insufficient immobilization of the triskelion to the substrate combined with exposure to shear forces may have caused a distortion of the legs.

The diameters of the legs differ depending on their orientation relative to the direction of the scan. Leg I in Fig. 3F was oriented parallel to the fast-scan axis. Its very low diameter of 2.0 to 3.5 nm results from the fact that the tip was 'riding' on top of the backbone. In contrast, leg III was immobilized perpendicular to the fast-scan axis; its width fluctuated between 4 and 12 nm. Possibly, only a few lysine residues had reacted with the underlying monolayer, which resulted in relatively movable sections. Leg II was sited with an angle of 25° to the fast-scan axis; it showed a more condensed appearance with an apparent width of 4 to 6 nm.

Further investigations to image in vitro prepared triskelia and to follow the in situ reassembly are currently in progress, as well as SFM experiments in the 'noncontact' mode in aqueous buffers. The SFM images presented here are the first ones of clathrin. Their remarkable quality (with the limitations indicated above) show that it is possible to follow in situ the dynamics of disassembly, and perhaps assembly, of macromolecules in aqueous buffers and, potentially, in 'real time'. The number

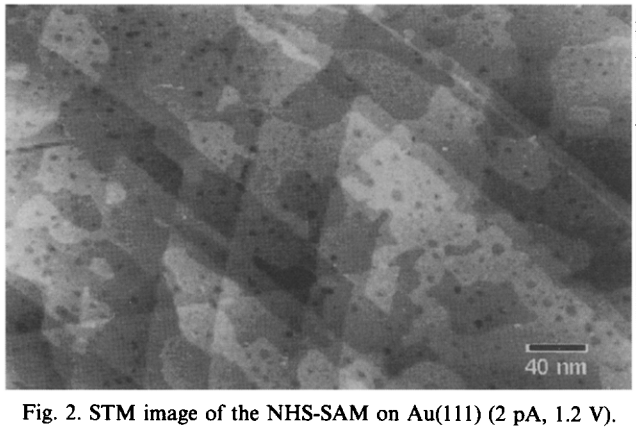

Fig. 2. STM image of the NHS-SAM on Au(111) (2 pA, 1.2 V).

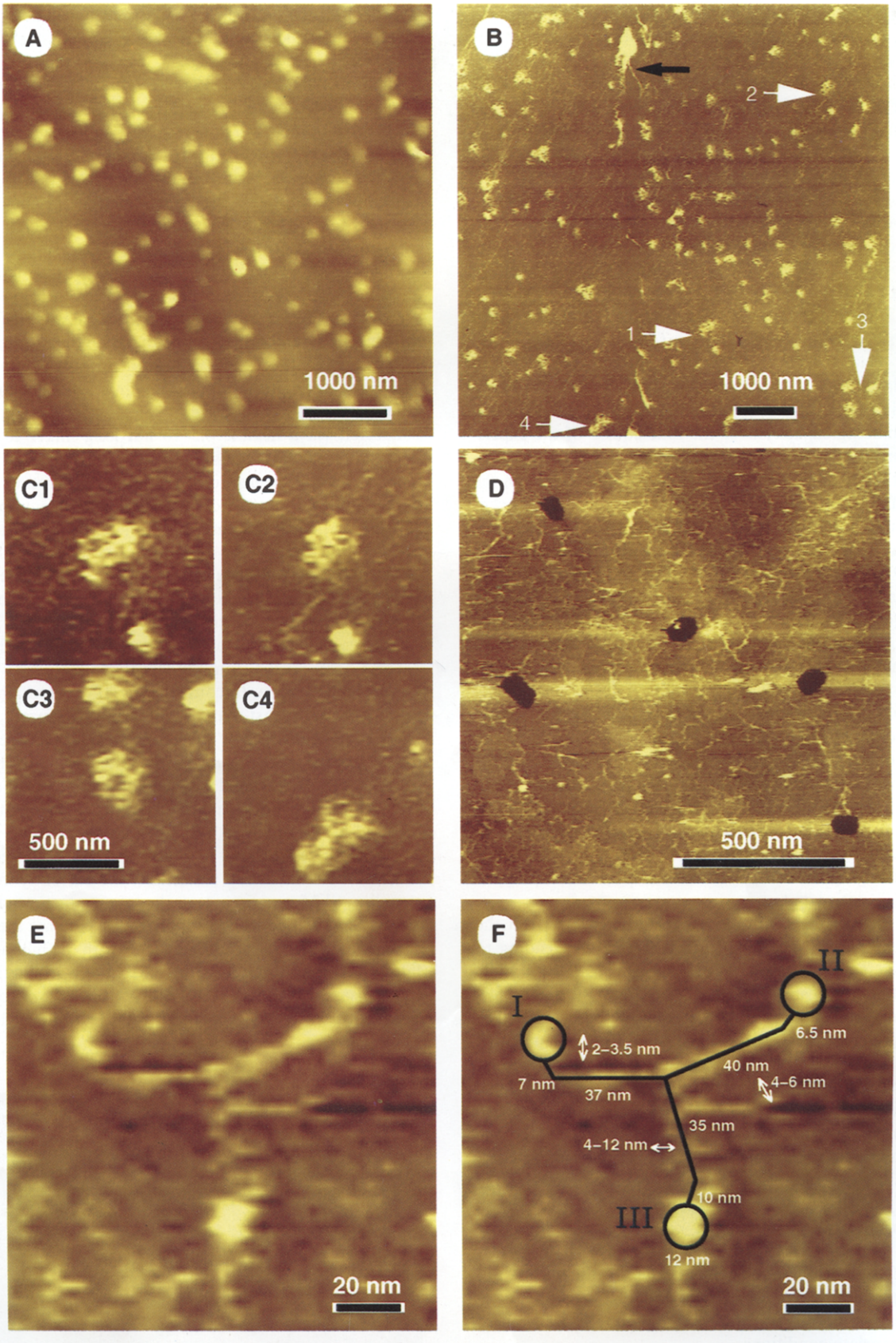
A
1000 nm
B
1
2
3
4
1000 nm
C1
C2
C3
C4
500 nm
D
500 nm
E
20 nm
F
I
II
III
2–3.5 nm
6.5 nm
40 nm
4–6 nm
7 nm
37 nm
35 nm
4–12 nm
10 nm
12 nm
20 nm

Fig. 3. SFM images of clathrin cages and triskelia, covalently bound to the *N*-hydroxysuccinimide-terminated SAM of Fig. 1, in aqueous buffers at room temperature. (A) Clathrin cages (1 μg/ml) in 0.1 M MES (pH 6.5), 0.5 mM $MgCl_2$, 1 mM EGTA, 0.02% NaN_3. The height of the cages was 16 ± 6 nm. (B) As in Fig. 3A, but 10 min after the exchange of the buffer, now in 0.5 M Tris-HCl (pH 7.0). The structures indicated by the white arrows are enlarged in Fig. 3C. For the black arrow, see text. (C) Magnified images of the four baskets indicated by the white arrows in Fig. 3B. The height of the baskets was approximately 2 nm. (D) Approx. 2 h after the exchange of buffer to Tris, pH 7; the cages have completely disassembled into individual triskelia. The black spots are holes in the gold film (see text). (E and F) A regularly spread out triskelion, with the dimensions indicated (F).
←

of observed dynamic processes of biological structures at the molecular level in the imaging mode of SPMs is still very small, e.g. the polymerization of fibrinogen [36]. Most investigations published on dynamic events deal, however, with much larger objects, such as platelets (measurement of their viscoelastic properties) [37], or pox virus particles (extrusion from kidney cells) [38].

The presented work paves the way for detailed investigations on the components involved in the formation and the disassembly of clathrin cages, such as adaptins and uncoating factors. More generally, we show that native macromolecules in aqueous buffers can be anchored covalently to an appropriate substrate, of which the *N*-hydroxysuccinimide derivative of Fig. 1 is just an example. It should be noted that the technique used to obtain the images of Fig. 3 is simple, rapid and reproducible.

Acknowledgements: This work was supported in part by special grants from the Swiss Federal Institute of Technology (ETH) Zurich, and the Schweizerische Krebsliga. E.U. was supported by start up funds from the Department of Pathology at the Washington University in St. Louis, MO. Thanks are also due to Prof. H.-J. Güntherodt, University of Basle, and to Dr. N. Mantei, ETH Zürich, for their suggestions and help.

References

[1] Engel, A. (1991) Annu. Rev. Biophys. Biophys. Chem. 20, 79–108.
[2] Yang, J., Tamm, L.K., Somlyo, A.P. and Shao, Z. (1993) J. Microsc. 171, 183–198.
[3] Hansma, H.G. and Hoh, J.H. (1994) Annu. Rev. Biophys. Biomol. Struct. 23, 115–139.
[4] Lal, R. and John, S.A. (1994) Am. J. Physiol. 266, C1–C21.
[5] Morris, V.J. (1994) Prog. Biophys. Mol. Biol. 61, 131–185.
[6] Yang, J., Mou, J. and Shao, Z. (1994) Biochim. Biophys. Acta 1199, 105–114.
[7] Schaper, A., Starink, J.P.P. and Jovin, T.M. (1994) FEBS Lett. 355, 91–95.
[8] Hansma, H.G., Bezanilla, M., Zenhäusern, F., Adrian, M. and Sinsheimer, R.L. (1993) Nucleic Acids Res. 21, 505–512.
[9] Thundat, T., Allison, D.P., Warmack, R.J., Brown, G.M., Jacobson, K.B., Schrick, J.J. and Ferrell, T.L. (1992) Scanning Microsc. 6, 911–918.
[10] Lyubchenko, Y.L., Oden, P.I., Lampner, D., Lindsay, S.M. and Dunker, K.A. (1993) Nucleic Acids Res. 21, 1117–1123.
[11] Butt, H.-J., Downing, K.H. and Hansma, P.K. (1990) Biophys. J. 58, 1473–1480.
[12] Karrasch, S., Dolder, M., Schabert, F., Ramsden, J. and Engel, A. (1993) Biophys. J. 65, 2437–2446.
[13] Heckl, W.M., Kallury, K.M.R., Thompson, M., Gerber, C., Hörber, H.J.K. and Binnig, G. (1989) Langmuir 5, 1433–1435.
[14] Clemmer, C.R. and Beebe, T.P., Jr. (1991) Science 251, 640–642.
[15] Heckl, W.M. and Binnig, G. (1992) Ultramicroscopy 42–44, 1073–1078.
[16] Nuzzo, R.G. and Allara, D.L. (1983) J. Am. Chem. Soc. 105, 4481–4483.
[17] Porter, M.D., Bright, T.B., Allara, D.L. and Chidsey, C.E.D. (1987) J. Am. Chem. Soc. 109, 3559–3568.
[18] Laibinis, P.E. and Whitesides, G.M. (1992) J. Am. Chem. Soc. 114, 1990–1995.
[19] Sellers, H., Ulman, A., Shnidman, Y. and Eilers, J.E. (1993) J. Am. Chem. Soc. 115, 9389–9401.
[20] Hegner, M., Wagner, P. and Semenza, G. (1993) Surf. Sci. 291, 39–46.
[21] Wagner, P., Hegner, M., Güntherodt, H.-J. and Semenza, G. (1995), to be submitted.
[22] Clemmer, C.R. and Beebe, T.B., Jr. (1992) Scanning Microsc. 6, 319–333.
[23] Hegner, M., Wagner, P. and Semenza, G. (1993) FEBS Lett. 336, 452–456.
[24] Rabke-Clemmer, C.E., Leavitt, A.J. and Beebe, T.P., Jr. (1994) Langmuir 10, 1796–1800.
[25] Leggett, G.J., Roberts, C.J., Williams, P.M., Davies, M.C., Jackson, D.E. and Tendler, S.J.B. (1993) Langmuir 9, 2356–2362.
[26] Lang, H., Duschl, C. and Vogel, H. (1994) Langmuir 10, 197–210.
[27] Häussling, L., Michel, B., Ringsdorf, H. and Rohrer, H. (1991) Angew. Chem. Int. Ed. Engl. 30, 569–572.
[28] Vigers, G.P., Crowther, R.A. and Pearse, B.M. (1986) EMBO J. 5, 529–534.
[29] Crowther, R.A., Finch, J.T. and Pearse, B.M. (1976) J. Mol. Biol. 103, 785–798.
[30] Keen, J.H., Willingham, M.C. and Pastan, I. (1979) Cell 16, 303–312.
[31] Campbell, C., Squicciarini, J., Shia, M., Pilch, P. and Fine, R. (1984) Biochemistry 23, 4420–4426.
[32] Schönenberger, C., Sondag-Huethorst, J.A.M., Jorritsma, J. and Fokkink, L.G.J. (1994) Langmuir 1994, 10, 611–614.
[33] Anselmetti, D., Baratoff, A., Güntherodt, H.-J., Delamarche, E., Michel, B., Gerber, Ch., Kang, H., Wolf, H. and Ringsdorf, H. (1994) Europhys. Lett. 27, 365–370.
[34] Jin, A.J. and Nossal, R. (1993) Biophys. J. 65, 1523–1537.
[35] Kocsis, E., Trus, B.L., Bisher, M.E. and Steven, A.C. (1991) J. Struct. Biol. 107, 6–14.
[36] Drake, B., Prater, C.B., Weisenhorn, A.L., Gould, S.A.C., Albrecht, T.R., Quate, C.M., Cannel, D.S., Hansma, H.G. and Hansma, P.K. (1989) Science 243, 1586–1589.
[37] Radmacher, M., Tillmann, R.W., Fritz, M. and Gaub, H.E. (1992) Science 257, 1900–1905.
[38] Hörber, J.K.H., Häberle, W., Ohnesorge, F., Binnig, G., Liebich, H.G., Czerny, C.Z., Mahnel, H. and Mayr, A. (1992) Scanning Microsc. 6, 919–930.

Note added in proof

After this work was completed, we became aware that a similar monolayer had been prepared by Nakano et al. (Anal. Sci. 9 (1993) 133–136), albeit by a different synthetic route and not for SPM purposes.